Electronic Supplementary Material (ESI) for New Journal of Chemistry.
This journal is © The Royal Society of Chemistry and the Centre National de la Recherche Scientifique 2015

Facile Synthesis of Shape-Controlled Graphene/Polyaniline Composites for High Performance Supercapacitor Electrode Materials

Xiaomiao Feng,*[1a] Ningna Chen,[1a] Jinhua Zhou, [a] Yi Li, [a] Zhendong Huang, [a] Lei Zhang, [a] Yanwen Ma,* [a] Lianhui Wang, [a] and Xiaohong Yan [b]

(a) Key Laboratory for Organic Electronics and Information Displays & Institute of Advanced Materials, National Jiangsu Syngerstic Innovation Center for Advanced Materials (SICAM), (b) College of Electronic Science and Engineering, Nanjing University of Posts & Telecommunications, 9 Wenyuan Road, Nanjing 210023, China

E-mail addresses: iamxmfeng@njupt.edu.cn, iamywma@njupt.edu.cn

Key Laboratory for Organic Electronics & Information Displays, Institute of Advanced Materials, School of Materials Science & Engineering, Nanjing University of Posts and Telecommunications, Nanjing 210046, China.

E-mail: iamxmfeng@njupt.edu.cn; iamywma@njupt.edu.cn

1. The SEM images of the cone shape growth

Fig.S1 exhibits the SEM images of the cone shapes of GPC-1 (A) and GPC-2 (B). As can be seen from the figure, with the decrease of the amount of aniline monomer, the cone becomes smaller.

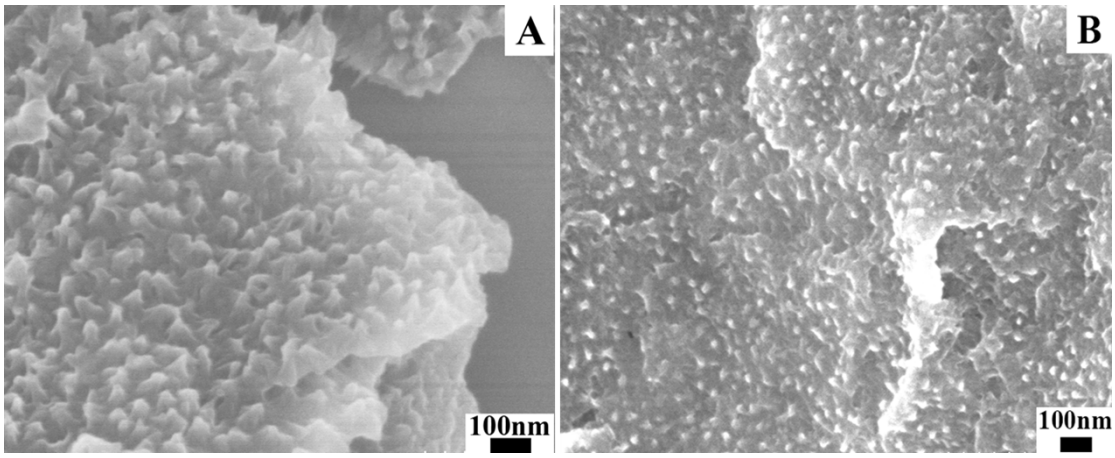

Fig.S1 The SEM images of the cone shapes of GPC-1 (A) and GPC-2 (B).

2. Electrochemical impedance spectroscopy

To understand capacitive behavior of the composites electrode materials well, the Nyquist plots of GPW-1, GPC-1, GPW-2, and GPC-2 have been tested. As shown in Fig.S2, EIS were collected within a frequency range of 0.01 Hz–100 kHz and voltage amplitude of 5 mV. The Nyquist plots showed an arc shape in the high frequency region and then a straight line in the low frequency region. The straight line at low frequency region indicates a good capacitive behavior, representative of fast ion diffusion in the electrode material. The interfacial charge-transfer resistance was measured by fitting the Nyquist data with an equivalent circuit similar. The equivalent series resistances (ESR) of GPW-1, GPC-1, GPW-2, and GPC-2 were 0.65, 1.09, 2.41, and 2.43 Ω, respectively. These low ESR could be attributed to high conductivity of

the composites.

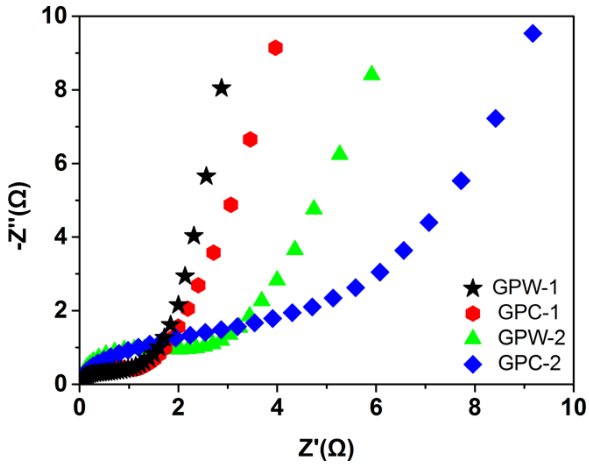

Fig.S2 Nyquist plots of GPW-1, GPC-1, GPW-2, and GPC-2 electrodes.

3. Zeta Potential data

The zeta potential measurement is performed by immersing the two electrodes in a cuvette consisting of the sample. If charged, the particles in the electric field will move with a specific velocity across the field lines toward the oppositely charged electrode. It can be seen from Fig.S3 clearly, GO solution (A) was negatively charged. On the basis of GO solution (A), the GO solution (B) was carried less negatively charge after magnetic stirring for 1h than that of original GO. The GO solution (C) was carried the least negatively charge among the three samples after sonication for 1h. These results proved that ultrasonic condition can accelerate the reduction process than stirring, which are in agreement with the reported work.[1, 2]

As we know, the collapse of cavitation bubbles generates localized high temperature (about 10^4 K), pressure (about 10^5 kPa) and cooling rates (in excess of 10^9 K s^{-1}) under ultrasonic condition, which can promote the reduction of GO. This condition cannot be obtained by stirring. So the reduction degree of GO is much higher by ultrasound treatment than that of stirring condition.

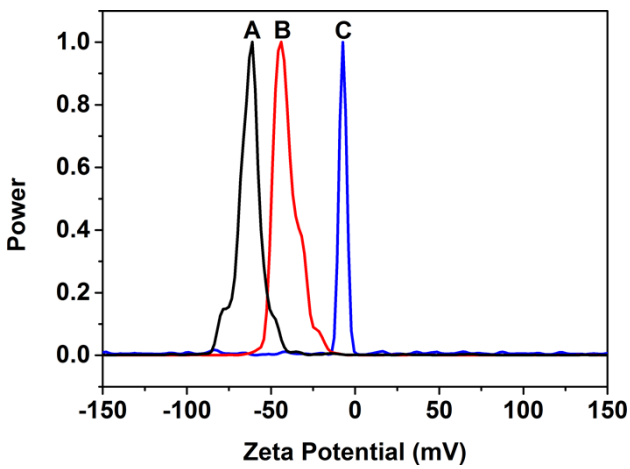

Fig.S3 Zeta Potential Power spectra of GO solution (A), stirred GO solution (B), and ultrasonic GO solution (C).

4. Coulombic efficiency

In Fig.5, the coulombic efficiency, referring to the ratio of discharge capacitance to charge capacitance, of GPW-1(a), GPC-1(b), GPW-2(c), and GPC-2(d) at a current density of 1.0 A/g was 85.4%, 42.6%, 35.9%, and 25.8%, respectively. This may be caused by the more loading and more effective utilization of PANI, the specific capacitance and coulombic efficiency of GPW-1 composite are both higher than those of other composites.[3] In Fig.7, the corresponding coulombic efficiency of GPW-1 composite at different current densities of 0.1, 0.5, 1.0, 2.0, 3.0, 4.0, and 5.0 A/g was 99.8%, 93.1%, 85.4%, 83.1%, 82.5%, 81.9%, and 80.2%, respectively. The coulombic efficiency decreased with the charge/discharge current density increased. The electrolyte ions could enter into the internal structure of the electro-active material well at lower current density, which resulting in low resistance and high coulombic efficiency.

4. Raman spectroscopy

Fig.S4 shows the Raman spectra of GO (A), GPW-1(B), and GPW-2(C). As shown in Fig.S4A, GO displays two prominent Raman-active peaks at 1355 cm^{-1} assigned to the D mode corresponding to the structural defects and G band at 1591 cm^{-1} related to the vibration of sp2-hybridized carbon. The characteristic bands of PANI, such as 1172 cm^{-1} band attributed to the in-plane C–H bending of quinoid units, 1335 cm^{-1} band assigned to $C–N^{+\cdot}$ stretching, and the band at 1597 cm^{-1} representing C=C stretching of the quinoid units could be clearly observed in Raman spectroscopy of GPW-1(B) and GPW-2(C). [4] This is probably due to the doping of carboxyl acid of GO to PANI backbone and π-π stacking of PANI and GO sheets. The result reveals that PANI was also in a doped state in the composite, and this observation was also supported by the XPS analysis and UV-vis absorption spectra.

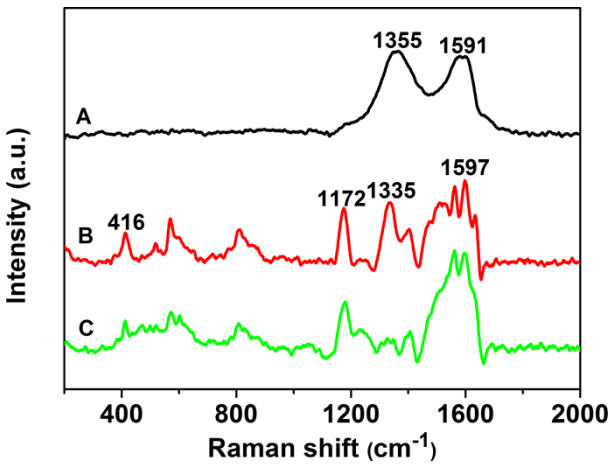

Fig.S4 Raman spectra of GO (A), GPW-1(B), and GPW-2(C).

5. Transmission electron microscopy (TEM) image

In order to study the detail morphology, TEM was utilized to describe the morphology of graphene/PANI composites. It was shown in Fig.S5A, lots of PANI nanowires were adsorbed on the graphene sheet uniformly. When the GO solution was

experienced one hour ultrasonication before hydrothermal treatment, the graphene/PANI nanocones were obtained, as revealed in Fig. S5B.

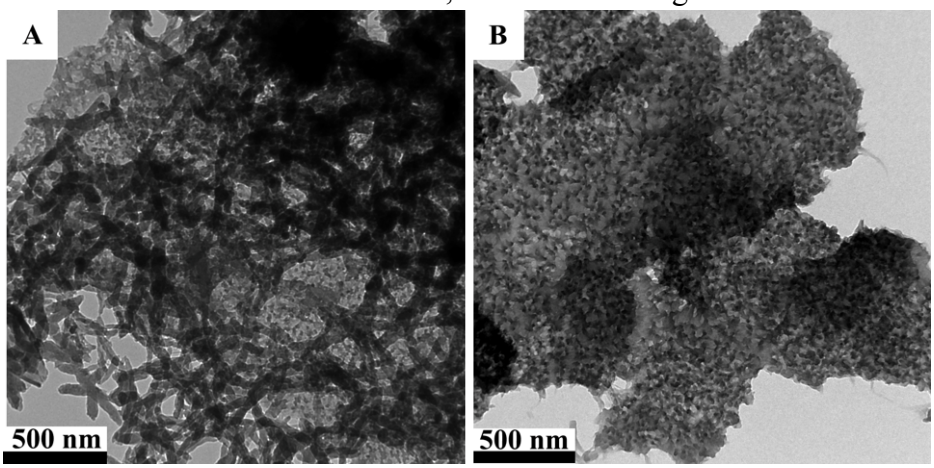

Fig.S5 TEM images of GPW-1(A) and GPC-1(B).

References

1 V. Loryuenyong, K. Totepvimarn, P. Eimburanapravat, W. Boonchompoo, and A. Buasri, *Adv Mater Sci Eng*, 2013, DOI: 10.1155/2013/923403.

2 W.-N. Zhang, W. He, and X.-L. Jing, *J. Phys. Chem.B*, 2010, **114**, 10368-10373.

3 Y.-Z. Li, X. Zhao, P.-P. Yu, and Q.-H. Zhang, *Langmuir*, 2013, **29**, 493-500.

4 X.-N. Chen, F.-C. Meng, Z.-W. Zhou, X. Tian, L.-M. Shan, S.-B. Zhu, X.-L. Xu, M. Jiang, L. Wang, D. Hui, Y. Wang, J. Lu, and J.-H. Gou, *Nanoscale*, 2014, **6**, 8140-8148.